厚生労働科学研究費補助金（難治性疾患克服研究事業）
分担研究報告書

Prader－Willi 症候群における諸症状の評価と治療効果の判定

研究分担者　村上信行　獨協医科大学越谷病院小児科

研究要旨

Prader-Willi 症候群（PWS）は、多様な症状を呈する先天奇形症候群である。われわれは、昨年度に引き続き、精神症状、側弯症、脂質代謝異常症について検討した。精神症状では、セロトニン再吸収阻害剤，ブチロフェノン系剤，セロトニン・ドーパミン拮抗薬（SDA）の有用性が示唆された。側弯症では、傍脊柱筋の増大率・左右差を検討することで側弯症の増悪を予測することができることが判明した。脂質代謝異常症では、GH 療法の良好な効果が示唆された。これらのデータは、Prader－Willi 症候群における治療指針の作成に大きく貢献すると期待される。

共同研究者
坂爪悟、田中百合子　獨協医科大学越谷病院小児科

A．研究目的

Prader-Willi 症候群（PWS）は、多様な症状を呈する先天奇形症候群である。われわれは、昨年度に引き続き、精神症状、側弯症、脂質代謝異常症について検討した。

B．研究方法

- 精神症状：　1998 年以降，濁協医大越谷病院小児科で診療した PWS 愚見 190 名の診療録を調査した．向精神病薬を用いた患者について，後方視的に検討した．
- 側弯症：対象は、当科において外来フォロー中の PWS 症候群患者で GH 療法を行い、定期的に側弯症のフォローおよび体組成評価のため腹部 CT scan を行うことができた 35 名である。年齢は 2 歳から 16 歳（中央値 3 歳）。男性 22 名、女性 13 名。欠失型（D）23 名、片親性ダイソミー（U）12 名。GH 療法開始年齢は 0 歳から 13 歳（中央値 3 歳）。観察期間は 6 ヵ月から 41 ヵ月（中央値 26 ヵ月）（表）。本研究で使用した腹部 CT 写真は、GH 療法による体組成の改善を評価するために撮影されたものであり、本研究のため撮影されたものではない。具体的には、6 ヵ月毎に脊椎 X 線写真をとり、Cobb 角 10 度以上を側弯とした。体組成評価のため腹部 CT scan を行い、そのフィルムを用いて傍脊柱筋の面積を測定した。傍脊柱筋の増大率[{latest total muscle volume－first total muscle volume} x 100]/ {first total muscle volume x period of observation (year)}とその左右差{(larger muscle volume－smaller muscle volume) x 100} / smaller muscle volume として、それぞれについて検討した。
- 脂質代謝異常症：対象は成長ホルモン療法中の 53 例。（男児　33 例，　女児　20 例、GH 療法開始時年齢　：中央値 3.5 歳　(0.7- 14.1)）GH 療法導入前、6 ヵ月後、1 年後における脂質（Tcho、TG、LDL、HDL）、HbA1C、HOMA-R、体組成の変化を後方視的に調べた。GH が脂質に及ぼす短期的影響と、最終経過観察時（1.0～9.6 年、中央値 4.6 年）までの長期的影響につき検討した。

表：臨床経過

患者	年齢	性	遺伝型	GHの開始年齢	観察開始年齢	観察期間	筋増大率	開始時の筋左右差	開始後の筋左右差
無側弯群									
1	3	M	D	0	0	22	73.0	4.9	5.7
2	4	M	U	0	1	32	75.5	13.2	6.9
3	4	M	D	0	1	37	93.5	9.6	2.6
4	6	F	D	0	5	14	10.9	10.4	1.4
5	3	M	U	1	1	12	36.7	7.9	3.0
6	5	F	D	1	1	30	28.8	4.3	7.1
7	3	M	U	1	1	18	83.7	17.2	5.7
8	2	M	D	1	1		64.3	5.7	0.7
9	3	M	U	1	1	6	39.0	6.8	1.1
10	3	F	D	1	1	10	114.1	12.3	6.3
11	14	F	D	1	10	31	8.8	3.6	5.2
12	3	F	D	2	1	10	65.5	6.6	1.5
13	5	M	D	2	1	21	32.1	2.1	4.8
14	3	M	D	2	2	9	45.3	0.4	7.6
15	7	F	D	3	6	9	34.5	7.0	7.7
16	14	M	D	4	8	32	11.0	5.1	2.1
17	13	M	D	5	9	38	23.4	12.2	4.2
18	13	F	U	5	11	15	12.5	5.4	4.3
19	9	M	U	7	7	11	12.8	6.3	5.0
20	11	F	D	7	8	29	11.1	10.5	2.9
21	6	F	D	8	3	18	34.7	10.2	0.8
22	15	M	U	9	12	29	8.6	22.8	3.9
無変化群									
1	4	F	U	1	2	27	47.8	6.5	0.8
2	10	M	D	1	6	36	8.0	12.2	8.2
3	6	M	D	3	3	28	41.3	8.8	7.7
4	4	M	U	3	3	9	54.0	0.7	0.2
5	12	M	D	6	8	41	10.9	21.0	5.8
増悪群									
1	8	F	D	1	3	10	38.5	7.2	17.3
2	9	M	D	4	8	9	2.5	9.0	8.8
3	11	M	D	5	8	36	11.1	13.9	11..2
4	9	F	D	11	11	28	10.5	5.3	7.8
5	16	M	U	11	13	26	2.2	11.7	17.0
6	16	M	D	13	13	29	5.4	12.7	11.7
改善群									
1	8	M	D	3	3	40	58.8	0.7	2.1
2	6	F	U	3	3	41	27.8	5.3	6.0

（倫理面への配慮）個人名は公表されず、患者さんのプライバシーは守られている。

C．研究結果

- 精神症状：PWS 患者 190 名のうち 25 名に向精神薬が投与されていた．セロトニン再吸収阻害剤(SSRI)11 名，セロトニン・ドーパミン拮抗薬（SDA）9 名，併用 1 名であった．SSRI の処方開始年齢は平均 12．8 歳，SDA 処方開始年齢は 16．5 歳であった．とくにこの一年は SDA の投与開始が多く，5 名に処方が開始された．SDA 処方例の概略は以下である．1) 13 歳 Del 男性 放火・自転車盗む自分で警察に出頭。2) 18 歳 UPD 男性 恐怖・不安・不眠，家人にナイフが刺さっているという幻覚。3) 16 歳 UPD 男性 祖母にナイフで斬りつける（11 歳から衝動に対して SSRI 処方されていた）。4) 17 歳 Del 女性 不眠，抑鬱，幻覚，妄想，独り言。5) 17 歳 Del 男性 当初落ち着きのなさ，物忘れに SSRI 処方されたがほどなく TV ゲームをきっかけに幻覚・妄想出現しリスペリドン投与で軽快。
- 側弯症：
  ① 側弯症の臨床経過：35 名中 22 名は経過中に側弯は認められなかった（無側弯群）。年齢は 2 歳から 15 歳（中央値 6 歳）。GH 療法開始年齢は 0 歳から 12 歳（中央値 2 歳）。観察期間は 6 ヵ月から 38 ヵ月（中央値 18 ヵ月）。5 名では GH 開始前から側弯症が認められたが、経過中変化が認められなかった（無変化群）。年齢は 4 歳から 6 歳（中央値 6 歳）。GH 療法開始年齢は 2 歳から 8 歳（中央値 3 歳）。観察期間は 9 ヵ月から 41 ヵ月（中央値 28 ヵ月）6 名では GH 療法開始前から側弯症が認められ、経過中に増悪が認められた（増悪群）。年齢は 8 歳から 16 歳（中央値 10 歳）。GH 療法開始年齢は 1 歳から 13 歳（中央値 8 歳）。観察期間は 9 ヵ月から 36 ヵ月（中央値 27 ヵ月）。2 名では GH 開始前から側弯症が認められたが、経過中に側弯が改善した（改善群）。年齢は 6 歳、3 歳。GH 療法開始年齢はともに 3 歳。観察期間は 40 ヵ月、41 ヵ月（表）。
  ② 傍脊柱筋の増大率、左右差：傍脊柱筋の増大率は無側弯群では 8.8-114.1 %/year (中央値 34.6 %/year)、無変化では 0-54.0 %/year (中央値 41.3 %/year)、増悪群では 2-38.6 %/year (中央値 8.0 %/year)、改善群はそれぞれ 58.8、27.8 %/year であった。無側弯群と増悪群、無変化群と増悪群間で有意差が認められた（図１）。傍脊柱筋の左右差は開始時無側弯群では 0.4-22.8% (中央値 6.9%)、無変化群では 0.7-21.0% (中央値 8.8%)、増悪群では 5.3-13.9% (中央値 10.4%)、改善群ではそれぞれ 0.7%、5.3%であった。これに対して観察終了時では 0.7-7.7% (中央値 4.3%)、無変化群では 0.2-8.2% (中央値 5.8%)、増悪群では 7.8-17.3% (中央値 11.7%)、改善群ではそれぞれ 1.8%、5.0%であった。観察期間中に無側弯群と無変化群では優位に左右差が減少した（図 2)。

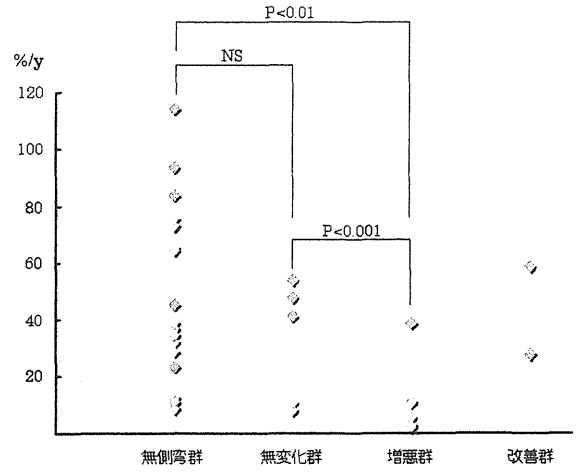

図1: 傍脊柱筋の増大率

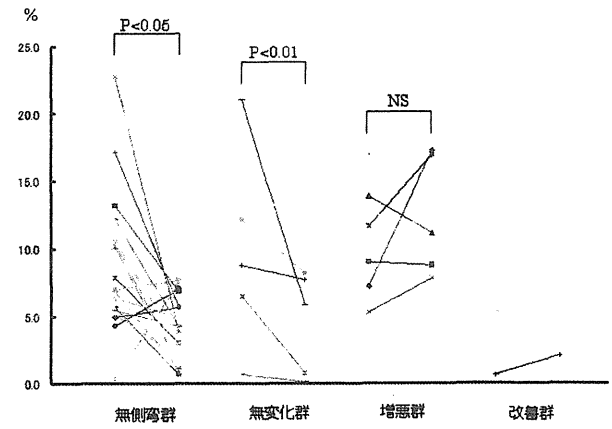

図2: 傍脊柱筋の左右差

- 脂質代謝異常症：ＧＨ投与前の脂質プロファイルは、中央値 Tcho 192.0mg/dl, TG 78.0mg/dl,LDL 117.0mg/dl, HDL 52.0mg/dl と正常であった。BMI は 17.1（12.5 - 32.5）、%FAT は 33.9%（10.2 -56.5）であった。 投与前、後における脂質パラメータの推移は、統計的有意差はないものの、Tcho (中央値：192→184mg/dl)と LDL(中央値：117→107mg/dl) の減少と HDL の増加 (中央値：52→60 mg/dl) 傾向がみられた。TG に変化はなかった。投与前 Tcho が 210mg/dl 以上（以後高コレステロール群と定義する）であったのは 15 例 (28%)で、TCho と LDL が高値を示した。高コレステロール群においては、Tcho、LDL の減少、HDL の上昇傾向がより顕著にみられ Tcho は、前の値に対し半年後、最終経過観察時において、P<0.05 の有意差をもって減少した。Tcho (中央値 : 224→204 mg/dl),LDL(中央値 : 160→126 mg/dl), HDL(中央値：47→56 mg/dl)。

脂質パラメータ推移まとめ（median）

全体（n=53）

	前	半年後	1年後	最終	
Tcho	192	187	185	184	↓
LDL	117	112	108	107	↓
TG	78	84	70	76	
HDL	52	56	56	60	↑

高コレステロール群（n=15）

Tcho	224	216*	210	204*	↓
LDL	160	143	138	126	↓
TG	90	100	100	98	
HDL	47	52	56	56	↑

*前の値に対しp<0.05
その他は統計的有意差なし

ＧＨ投与後、％ＦＡＴは有意に減少し(P<0.001)、体組成の改善が見られた。投与前においても投与後においても脂質のパラメータと%FAT とは相関がなかった。また投与前と投与後 6 ヵ月後において、Tcho と％FAT の変化率には相関がなかった。 インスリン抵抗性はＧＨ投与により増加した（p<0.05）。中央値は(0.9→1.6)と正常範囲内であった。HbA1C は前後で変化しなかった。前に HbA1C 高値（>6.5%）を呈していた 2 例も改善し、最終経過観察時までに糖尿病は発症していない。糖尿病発症は投与後 7 年経過した摂食コントロール不良の 1 例のみにみられた。

Ｄ．考察

● 精神症状：今回は心理検査，知能検査などは検討できていないが向精神病薬が PWS 患者のＱＯＬに一定の効果があるとの印象が持てる． SSRI は学童期に有用であり，投与開始により “焦燥""パニック""盗食"に有効であった．また，投与開始後から“作業所に通うことが楽しい"など，抑鬱の改善も見られた．また，思春期以降に見られる非定型精神病症状，幻覚・せん妄には SDA が有効であり，急性期に著効する．しかし，その後の他剤への変更投与や環境整備が必須である．一部症例では“ブチロフェノン系薬剤を開始して人が変わった”と家人の声もきかれた．しかし，向精神病薬の内服を開始したものの，なかなか社会生活に溶け込めない患者もいる．このような患者の共通点は，環境整備ができていない．さらに，幼少期から家族の協力が得られない場合や，環境が整備されない場合は向精神病薬の効果が得られない．

SSRI は従来から取り入れた薬剤でセロトニン再吸収阻害剤である．一般臨床ではおもに鬱病やパニック障害に使用されている．PWS の特有なしつこさ，パニックに対して当院では SSRI を使用している．PWS 欠失領域にある SNORNA がセロトニン伝達経路に関与することから，PWS の精神症状の軽減に有望と考えている．10 代半ばから成人期にかけて幻覚・妄想を前景にした統合失調症様の非定型精神症状が見られる．独り言が多く，理解できない発言や行動に家族は悩み，時に凶暴な行為に家族の身体的な危機にさらされる．非欠失型（UPD）による PWS 患者に見られる傾向があり．SDA が有効であり，環境調整によりほとんどの患者で減薬・休薬ができる．統合失調症の遺伝学的検査で PWS 領域近傍の欠失・重複は複数の報告があり，共通した機序が考えられる．

● 側弯症：

側弯症の臨床経過：GH 療法開始時に側弯症のない22名のPWS症候群患者では側弯症を発症しなかった。これに対して GH 療法開始時に側弯症のあった患者13名中側弯症の変化のないもの5名、増悪したもの6名、そして2名に改善がみられた。対象患者35名中13名に側弯症の合併が認められ、37．1%であった。この側弯症合併の頻度はこれまでに報告された頻度と比較して低く、GH 療法が側弯症の合併頻度を上昇させてはいなかった。しかしながら、今回の対象患者年齢が低いため、さらに検討する必要があると考えられた。

側弯症増悪群では、GH 療法開始年齢が遅く、中央値は 8 歳であった。これに対して、側弯症無変化群、無側弯群ではそれぞれ中央値 3 歳、2 歳。対象患者人数も少なく、今回のみの検討では GH 療法開始年齢が遅いことが側弯症合併のリスクとなるか否かについて結論を出すことは困難であるが、GH 療法を開始するのであれば、開始年齢が早いほうがよいと考えられた。また、観察開始時に側弯症を合併したにもかかわらず、2 名に GH 療法中に側弯症の改善がみられたことは大変興味深いものである。側弯症改善群においても GH 療法開始年齢はともに 3 歳と側弯症増悪群に比較して早いものであった。

遺伝子型では、通常臨床症状は欠失型が片親性ダイソミーに比較して重いとされている。開始時側弯症の合併がみられた 13 名中 8 名（69．2%）が欠失型であり、PWS 患者における遺伝子型の比率と比較して高いものではなかった。遺伝子型による側弯症の合併頻度の差は認められなかった。側弯増悪群では 6 名中 5 名が欠失型であり、比較的欠失型の患者が多かった。しかし、対象患者数が少なく、今後の検討が必要であると考えられた。

② 傍脊柱筋の増大率、左右差

筋の断面積は筋力に比例する。筋の増大率は筋力の増加を示す。また、筋の断面積の左右差は筋力のアンバランスを示す。傍脊柱筋の増大率を各群間で検討すると増悪群では、傍脊柱筋の増大率が無側弯群や無変化群に比較して有意に低かった。しかし、筋増大率は年齢とともに低下する傾向があり、増悪群患者の年齢が無側弯群や無変化群に比較して高いことから簡単に筋増大率を比較することではできない。年齢をあわせて比較するとは困難であるが、側弯増悪群で低い傾向はみられた。今後さらに対象患者数を増やし、検討する、または正常者の筋増大率を検討する必要があると考えられた。

また、観察期間での傍脊柱筋の左右差について検討すると無側弯群や無変化群では筋の左右差が有意に改善するのに対して増悪群では左右差の

改善が認められなかった。傍脊柱筋の左右差に関しては、側弯症による二次的変化ではないかと考えられたが、無側弯群においても左右差がみられ改善することと側弯症の型が同じであるにも関わらず、面積の小さい筋（または大きい筋）の左右がかならずしも一定でないことから本症にみられる傍脊柱筋の左右差は側弯症による二次的変化ではないものと考えられた。これらのことからGH療法中に傍脊柱筋の筋力のアンバランス改善されなかった場合に側弯症が進行する傾向があると考えられた。

- 脂質代謝異常症：ＧＨ投与により、特に高コレステロール群においてTcho、LDLの減少がみられ、脂質環境の改善がみられた。GHによる体組成の改善度と高脂血症の改善度とは相関がみられず、LDL レセプターの増加など、他の因子が関与していると思われた。PWS における高脂血症の一因にgrowth hormone deficiencyの関与が示唆された。一般的にＧＨによりインスリン抵抗性が増加すると言われているが、検討症例においてHbA1Cは変化せず、GH導入を疇躇するような有害事象とはなっていなかった。PWS において、高脂血症の改善は心血管系疾患のリスクを減らし、生命予後を左右する可能性もあり、ＧＨ療法は積極的に導入するべきと考えた。尚、今回の研究対象においても、ＧＨ投与前における%FATやＢＭＩと高脂血症との間に相関はなかった。BMIをマッチングさせた単純性肥満に比し、ＰＷＳの高脂血症やインスリン抵抗性は軽度であると報告されている。内臓脂肪から分泌されるアディポサイトカインのうち、TNF -α、CRP、レプチン、レジスチンなどは、心血管系に慢性炎症を起こし、糖代謝、脂質代謝にも作用し、いわゆるメタボリック症候群を惹起する物質である。これらのアディポサイトカインの過剰状態においては、高血圧、動脈硬化、インスリン抵抗性の増悪、高脂血症等を呈し、心血管系疾患を引き起こす。一方、やはりアディポサイトカインの一つであるアディポネクチンは、インスリン抵抗性を緩和し、動脈硬化を防ぐなど心血管系に有利な方向に働く物質である。
近年、PWSの高アディポネクチン血症を指摘した論文が散見される。今後、アディポネクチンはじめ、アディポサイトカインがＰＷＳの脂質代謝やインスリン抵抗性とどう関連しているか、またＧＨ投与により、どのように変化していくのか検討する予定である。

Ｅ．結論

Prader-Willi症候群（PWS）は、多様な症状を呈する先天奇形症候群である。われわれは、昨年度に引き続き、精神症状、側弯症、脂質代謝異常症について検討した。精神症状では、セロトニン再吸収阻害剤，ブチロフェノン系剤，セロトニン・ドーパミン拮抗薬（SDA）の有用性が示唆された。側弯症では、P傍脊柱筋の増大率・左右差を検討することで側弯症の増悪を予測することができることが判明した。脂質代謝異常症では、GH療法の良好な効果が示唆された。これらのデータは、Prader－Willi症候群における治療指針の作成に大きく貢献すると期待される。

Ｆ．健康危険情報

該当なし

Ｇ．研究発表

１．論文発表

２．学会発表

1. 城戸康宏、坂爪悟、村上信行、永井敏郎。プラダー・ウイリー症候群患者への男性ホルモン補充の効果。第33回日本小児遺伝学会。盛岡、4 22 2010
2. 坂爪悟、城戸康宏、村上信行、永井敏郎。獨協医科大学越谷病院にて加療中のプラダー・ウイリー症候群患者における向精神薬の使用状況。第33回日本小児遺伝学会。盛岡、4 22 2010
3. Nobuyuki Murakami, Hisashi Itabashi, Yuji Oto, Kazuo Obata, Toshiro Nagai； THE MEASUREMENT OF PARAVERTEBRAL MSUCLE VOLUME CAN BE A USEFUL INDICATOR OF PROGRESSION OF SCOLIOSIS IN PWS WITH GH THERAPY. 7th International Prader-Willi syndrome conference. Taipei Taiwan, 19-23, 2010
4. Toshiro Nagai, Yutaka Nakamura, Masataka Kakihana, Kazuo Obata, Satoru Sakazume, Nobuyuki Murakami.；FREQUENCY AND RISK FACTORS OF SEVERE SCOLIOSIS IN PRADER-WILLI SYNDROME. 7th International Prader-Willi syndrome conference. Taipei Taiwan, 19-23, 2010
5. Yuriko Tanaka, Nobuyuki Murakami, YUJI Oto, Hisashi Itabashi, Takayoshi Tsuchiya, Kazuo Obata, Toshiro Nagai.;GROWTH HORMONE THERAPY IMPROVES HYPERLIPIDEMIA IN CHILDREN WITH PRADER-WILLI SYNDROME. 7th International Prader-Willi syndrome conference. Taipei Taiwan, 19-23, 2010
6. Yasuhiro Kido, Kazuo Obata, Takayoshi Tsuchiya, Yuuzou Tomita, Nobuyuki Murakami, Toshiro Nagai.； TESTOSTERONE REPLACEMENT THERAPY IN 18 ADULT PATIENTS WITH PRADER-WILLI SYNDROME. 7th International Prader-Willi syndrome conference. Taipei
7. 第２３回小児脂質研究会(福岡)
「Prader-Willi 症候群（PWS)における成長ホルモン療法は高脂血症を改善する」
田中百合子、土屋貴義、村上信行、永井敏郎
8. 7th International PWS Conference (Taipei)２０１０
“Growth hormon therapy improves hyperlipidemia in Prader-Willi Sydrome”Yuriko Tanaka, Nobuyuki Murakami , Yuji Oto , Hisashi Itabashi , Takayoshi Tsuchiya , Kazuo Obata , Toshiro Nagai

H．知的財産権の出願・登録状況
（予定を含む。）

1．特許取得

2．実用新案登録

3．その他

別紙4

雑誌

発表者氏名	論文タイトル名	発表誌名	巻名	ページ	出版年
Matsubara K, Murakami N, Nagai T, Ogata T	Maternal age effect on the development of Prader-Willi syndrome resulting from upd(15)mat through meiosis 1 errors..	Hum Reprod (submitted)			2010
Kagami M, O'Sullivan MJ, Green AJ, Watabe Y, Arisaka O, Masawa N, Matsuoka K, Fukami M, Matsubara K, Kato F, Ferguson-Smith AC, Ogata T	The IG-DMR and the MEG3-DMR at human chromosome 14q32.2: hierarchical interaction and distinct functional properties as imprinting control centers.	PLoS Genet	6 (6)	e1000992	2010
Yamazawa K, Nakabayashi K, Kagami M, Sato T, Saitoh S, Horikawa R, Hizuka N, Ogata T	Parthenogenetic chimaerism/mosaicism with a Silver-Russell Syndrome-like Phenotype.	J Med Genet	47 (11)	782-785	2010
Suzumori N, Ogata T, Mizutani E, Hattori Y, Matsubara K, Kagami M, Suguhara-Ogasawara M	Prenatal diagnosis of paternal uniparental disomy 14: delineation of further patient.	Am J Med Genet A	152A (12)	3189-3192	2010
Yamazawa K, Nakabayashi K, Matsuoka K, Matsubara K, Hata K, Horikawa R, Ogata T	Androgenetic/biparental mosaicism in a girl with Beckwith-Wiedemann syndrome-like and upd(14)pat-like phenotypes.	J Hum Genet	56 (1)	91-93	2011
Yamazawa K, Ogata T, Ferguson-Smith AC	Uniparental disomy and human disease: an overview.	Am J Med Genet C	154C (3)	329-334	2010
Fukami M, Nagai T, Mochizuki H, Muroya K, Yamada G, Takitani K, Ogata T.	Anorectal and urinary anomalies and aberrant retinoic acid metabolism in cytochrome P450 oxidoreductase deficiency.	Mol Genet Metab	100 (3)	269-273,	2010

研究成果の刊行一覧表

研究成果の刊行物・別刷り

The IG-DMR and the *MEG3*-DMR at Human Chromosome 14q32.2: Hierarchical Interaction and Distinct Functional Properties as Imprinting Control Centers

Masayo Kagami[1], Maureen J. O'Sullivan[2], Andrew J. Green[3,4], Yoshiyuki Watabe[5], Osamu Arisaka[5], Nobuhide Masawa[6], Kentarou Matsuoka[7], Maki Fukami[1], Keiko Matsubara[1], Fumiko Kato[1], Anne C. Ferguson-Smith[8], Tsutomu Ogata[1]*

1 Department of Endocrinology and Metabolism, National Research Institute for Child Health and Development, Tokyo, Japan, 2 Department of Pathology, School of Medicine, Our Lady's Children's Hospital, Trinity College, Dublin, Ireland, 3 National Center for Medical Genetics, University College Dublin, Our Lady's Hospital, Dublin, Ireland, 4 School of Medicine and Medical Science, University College, Dublin, Ireland, 5 Department of Pediatrics, Dokkyo University School of Medicine, Tochigi, Japan, 6 Department of Pathology, Dokkyo University School of Medicine, Tochigi, Japan, 7 Department of Pathology, National Center for Child Health and Development, Tokyo, Japan, 8 Department of Physiology, Development and Neuroscience, University of Cambridge, Cambridge, United Kingdom

Abstract

Human chromosome 14q32.2 harbors the germline-derived primary *DLK1-MEG3* intergenic differentially methylated region (IG-DMR) and the postfertilization-derived secondary *MEG3*-DMR, together with multiple imprinted genes. Although previous studies in cases with microdeletions and epimutations affecting both DMRs and paternal/maternal uniparental disomy 14-like phenotypes argue for a critical regulatory function of the two DMRs for the 14q32.2 imprinted region, the precise role of the individual DMR remains to be clarified. We studied an infant with upd(14)pat body and placental phenotypes and a heterozygous microdeletion involving the IG-DMR alone (patient 1) and a neonate with upd(14)pat body, but no placental phenotype and a heterozygous microdeletion involving the *MEG3*-DMR alone (patient 2). The results generated from the analysis of these two patients imply that the IG-DMR and the *MEG3*-DMR function as imprinting control centers in the placenta and the body, respectively, with a hierarchical interaction for the methylation pattern in the body governed by the IG-DMR. To our knowledge, this is the first study demonstrating an essential long-range imprinting regulatory function for the secondary DMR.

Citation: Kagami M, O'Sullivan MJ, Green AJ, Watabe Y, Arisaka O, et al. (2010) The IG-DMR and the *MEG3*-DMR at Human Chromosome 14q32.2: Hierarchical Interaction and Distinct Functional Properties as Imprinting Control Centers. PLoS Genet 6(6): e1000992. doi:10.1371/journal.pgen.1000992

Editor: Wolf Reik, The Babraham Institute, United Kingdom

Received December 29, 2009; **Accepted** May 19, 2010; **Published** June 17, 2010

Funding: This work was supported by grants from the Ministry of Health, Labor, and Welfare; from the Ministry of Education, Science, Sports and Culture; and from Takeda Science Foundation. The funders had no role in study design, data collection and analysis, decision to publish, or preparation of the manuscript.

Competing Interests: The authors have declared that no competing interests exist.

* E-mail: tomogata@nch.go.jp

Introduction

Human chromosome 14q32.2 carries a cluster of protein-coding paternally expressed genes (*PEGs*) such as *DLK1* and *RTL1* and non-coding maternally expressed genes (*MEGs*) such as *MEG3* (alias, *GTL2*), *RTL1as* (*RTL1* antisense), *MEG8*, *snoRNAs*, and *microRNAs* [1,2]. Consistent with this, paternal uniparental disomy 14 (upd(14)pat) results in a unique phenotype characterized by facial abnormality, small bell-shaped thorax, abdominal wall defects, placentomegaly, and polyhydramnios [2,3], and maternal uniparental disomy 14 (upd(14)mat) leads to less-characteristic but clinically discernible features including growth failure [2,4].

The 14q32.2 imprinted region also harbors two differentially methylated regions (DMRs), i.e., the germline-derived primary *DLK1-MEG3* intergenic DMR (IG-DMR) and the postfertilization-derived secondary *MEG3*-DMR [1,2]. Both DMRs are hypermethylated after paternal transmission and hypomethylated after maternal transmission in the body, whereas in the placenta the IG-DMR alone remains as a DMR and the *MEG3*-DMR is rather hypomethylated [1,2]. Furthermore, previous studies in cases with upd(14)pat/mat-like phenotypes have revealed that epimutations (hypermethylation) and microdeletions affecting both DMRs of maternal origin cause paternalization of the 14q32.2 imprinted region, and that epimutations (hypomethylation) affecting both DMRs of paternal origin cause maternalization of the 14q32.2 imprinted region, while microdeletions involving the DMRs of paternal origin have no effect on the imprinting status [2,5–8]. These findings, together with the notion that parent-of-origin specific expression patterns of imprinted genes are primarily dependent on the methylation status of the DMRs [9], argue for a critical regulatory function of the two DMRs for the 14q32.2 imprinted region, with possible different effects between the body and the placenta.

However, the precise role of individual DMR remains to be clarified. Here, we report that the IG-DMR and the *MEG3*-DMR show a hierarchical interaction for the methylation pattern in the body, and function as imprinting control centers in the placenta and the body, respectively. To our knowledge, this is the first study demonstrating not only different roles between the primary and secondary DMRs at a single imprinted region, but also an essential regulatory function for the secondary DMR.

Author Summary

Genomic imprinting is a process causing genes to be expressed in a parent-of-origin specific manner—some imprinted genes are expressed from maternally inherited chromosomes and others from paternally inherited chromosomes. Imprinted genes are often located in clusters regulated by regions that are differentially methylated according to their parental origin. The human chromosome 14q32.2 imprinted region harbors the germline-derived primary *DLK1-MEG3* intergenic differentially methylated region (IG-DMR) and the postfertilization-derived secondary *MEG3*-DMR, together with multiple imprinted genes. Perturbed dosage of these imprinted genes, for example in patients with paternal and maternal uniparental disomy 14, causes distinct phenotypes. Here, through analysis of patients with microdeletions recapitulating some or all of the uniparental disomy 14 phenotypes, we show that the IG-DMR acts as an upstream regulator for the methylation pattern of the *MEG3*-DMR in the body but not in the placenta. Importantly, in the body, the *MEG3*-DMR functions as an imprinting control center. To our knowledge, this is the first study demonstrating an essential function for the secondary DMR in the regulation of multiple imprinted genes. Thus, the results provide a significant advance in the clarification of underlying epigenetic features that can act to regulate imprinting.

Results

Clinical reports

We studied an infant with upd(14)pat body and placental phenotypes (patient 1) and a neonate with upd(14)pat body, but no placental, phenotype (patient 2) (Figure 1). Detailed clinical features of patients 1 and 2 are shown in Table 1. In brief, patient 1 was delivered by a caesarean section at 33 weeks of gestation due to progressive polyhydramnios despite amnioreduction at 28 and 30 weeks of gestation, whereas patient 2 was born at 28 weeks of gestation by a vaginal delivery due to progressive labor without discernible polyhydramnios. Placentomegaly was observed in patient 1 but not in patient 2. Patients 1 and 2 were found to have characteristic face, small bell-shaped thorax with coat hanger appearance of the ribs, and omphalocele. Patient 1 received surgical treatment for omphalocele immediately after birth and mechanical ventilation for several months. At present, she is 5.5 months of age, and still requires intensive care including oxygen administration and tube feeding. Patient 2 died at four days of age due to massive intracranial hemorrhage, while receiving intensive care including mechanical ventilation. The mother of patient 1 had several non-specific clinical features such as short stature and obesity. The father of patient 1 and the parents of patient 2 were clinically normal.

Sample preparation

We isolated genomic DNA (gDNA) and transcripts (*mRNAs*, *snoRNAs*, and *microRNAs*) from fresh leukocytes of patients 1 and the parents of patients 1 and 2, from fresh skin fibroblasts of patient 2, and from formalin-fixed and paraffin-embedded placental samples of patient 1 and similarly treated pituitary and adrenal samples of patient 2 (although multiple body tissues were available in patient 2, useful gDNA and transcript samples were not obtained from other tissues probably due to drastic post-mortem degradation). We also made metaphase spreads from leukocytes and skin fibroblasts. For comparison, we obtained control samples from fresh normal adult leukocytes, neonatal skin fibroblasts, and placenta at 38 weeks of gestation, and from fresh leukocytes of upd(14)pat/mat patients and formalin-fixed and paraffin-embedded placenta of a upd(14)pat patient [2,3].

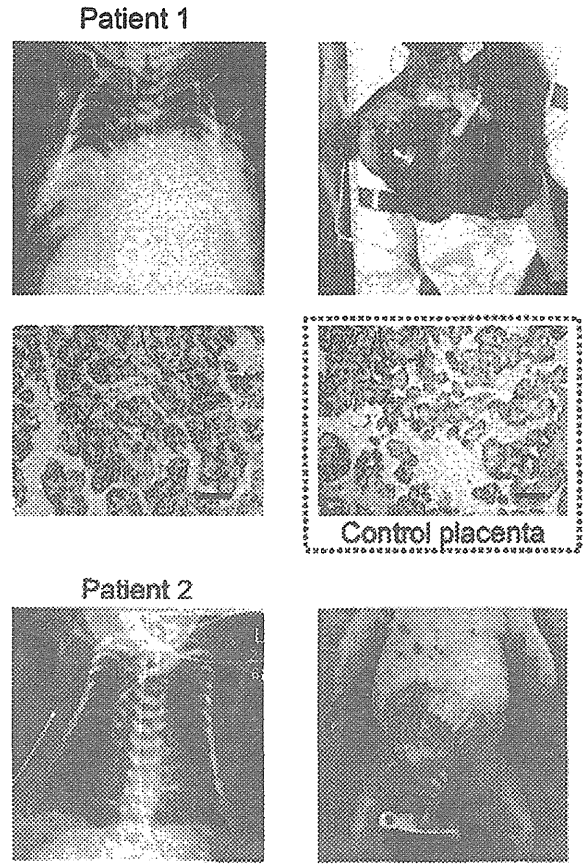

Figure 1. Clinical phenotypes of patients 1 and 2 at birth. Both patients have bell shaped thorax with coat hanger appearance of the ribs and omphalocele. In patient 1, histological examination of the placenta shows proliferation of dilated and congested chorionic villi, as has previously been observed in a case with upd(14)pat [2]. For comparison, the histological finding of a gestational age matched (33 weeks) control placenta is shown in a dashed square. The horizontal black bars indicate 100 μm.
doi:10.1371/journal.pgen.1000992.g001

Structural analysis of the imprinted region

We first examined the structure of the 14q32.2 imprinted region (Figure 2). Upd(14) was excluded in patients 1 and 2 as well as in the mother of patient 1 by microsatellite analysis (Table S1), and FISH analysis for the two DMRs identified a familial heterozygous deletion encompassing the IG-DMR alone in patient 1 and her mother and a *de novo* heterozygous deletion encompassing the *MEG3*-DMR alone in patient 2 (Figure 2). The microdeletions were further localized by SNP genotyping for 70 loci (Table S1) and quantitative real-time PCR (q-PCR) analysis for four regions around the DMRs (Figure S1A), and serial direct sequencing for the long PCR products harboring the deletion junctions successfully identified the fusion points of the microdeletions in patient 1 and her mother and in patient 2 (Figure 2). According to the NT_026437 sequence data at the NCBI Database (Genome Build 36.3) (http://preview.ncbi.nlm.nih.gov/guide/), the deletion

Table 1. Clinical features in patients 1 and 2.

	Patient 1	Patient 2	Upd(14)pat (n = 20)[c]
Present age	5.5 months	Deceased at 4 days	0–9 years
Sex	Female	Female	Male:Female = 9:11
Karyotype	46,XX	46,XX	
Pregnancy and delivery			
Gestational age (weeks)	33	28	28–37
Delivery	Caesarean	Vaginal	Vaginal:Caesarean = 6:7
Polyhydramnios	Yes	No	20/20 (<28)[d]
Amnioreduction (weeks)	2× (28, 30)	No	6/6
Placentomegaly	Yes	No	10/10
Growth pattern			
Prenatal growth failure	No	No	1/13
Birth length (cm)	43 (WNR)[a]	34 (WNR)[a]	
Birth weight (kg)	2.84 (>90 centile)[a]	1.32 (WNR)[a]	
Postnatal growth failure	Yes	…	5/6
Present stature (cm)	56.3 (−3.0 SD)[b]	…	
Present weight (kg)	5.02 (−3.0 SD)[b]	…	
Characteristic face			
Frontal bossing	No	Yes	5/7
Hairy forehead	Yes	Yes	9/10
Blepharophimosis	Yes	No	14/15
Depressed nasal bridge	Yes	Yes	13/13
Anteverted nares	Yes	No	6/10
Small ears	Yes	Yes	11/12
Protruding philtrum	Yes	No	15/15
Puckered lips	No	No	3/10
Micrognathia	Yes	Yes	11/12
Thoracic abnormality			
Bell-shaped thorax	Yes	Yes	17/17
Mechanical ventilation	Yes	Yes	17/17
Abdominal wall defect			
Diastasis recti	…	…	15/17
Omphalocele	Yes	Yes	2/17[e]
Others			
Short webbed neck	Yes	Yes	14/14
Cardiac disease	No	Yes (PDA)	5/10
Inguinal hernia	No	No	2/6
Coxa valga	Yes	No	3/4
Joint contractures	Yes	No	8/10
Kyphoscoliosis	No	No	4/7
Extra features		Hydronephrosis (bilateral)	

WNR: within the normal range; SD: standard deviation; and PDA: patent ductus arteriosus.

a Assessed by the gestational age- and sex-matched Japanese reference data from the Ministry of Health, Labor, and Welfare (http://www.e-stat.go.jp/SG1/estat/GL02020101.do).

b Assessed by the age- and sex-matched Japanese reference data..

c In the column summarizing the clinical features of 20 patients with upd(14)pat, the denominators indicate the number of cases examined for the presence or absence of each feature, and the numerators represent the number of cases assessed to be positive for that feature; thus, the differences between the denominators and the numerators denote the number of cases evaluated to be negative for that feature (adopted from reference [2]).

d Polyhydramnios has been identified by 28 weeks of gestation.

e Omphalocele is present in two cases with upd(14)pat and in two cases with epimutations [2].

doi:10.1371/journal.pgen.1000992.t001

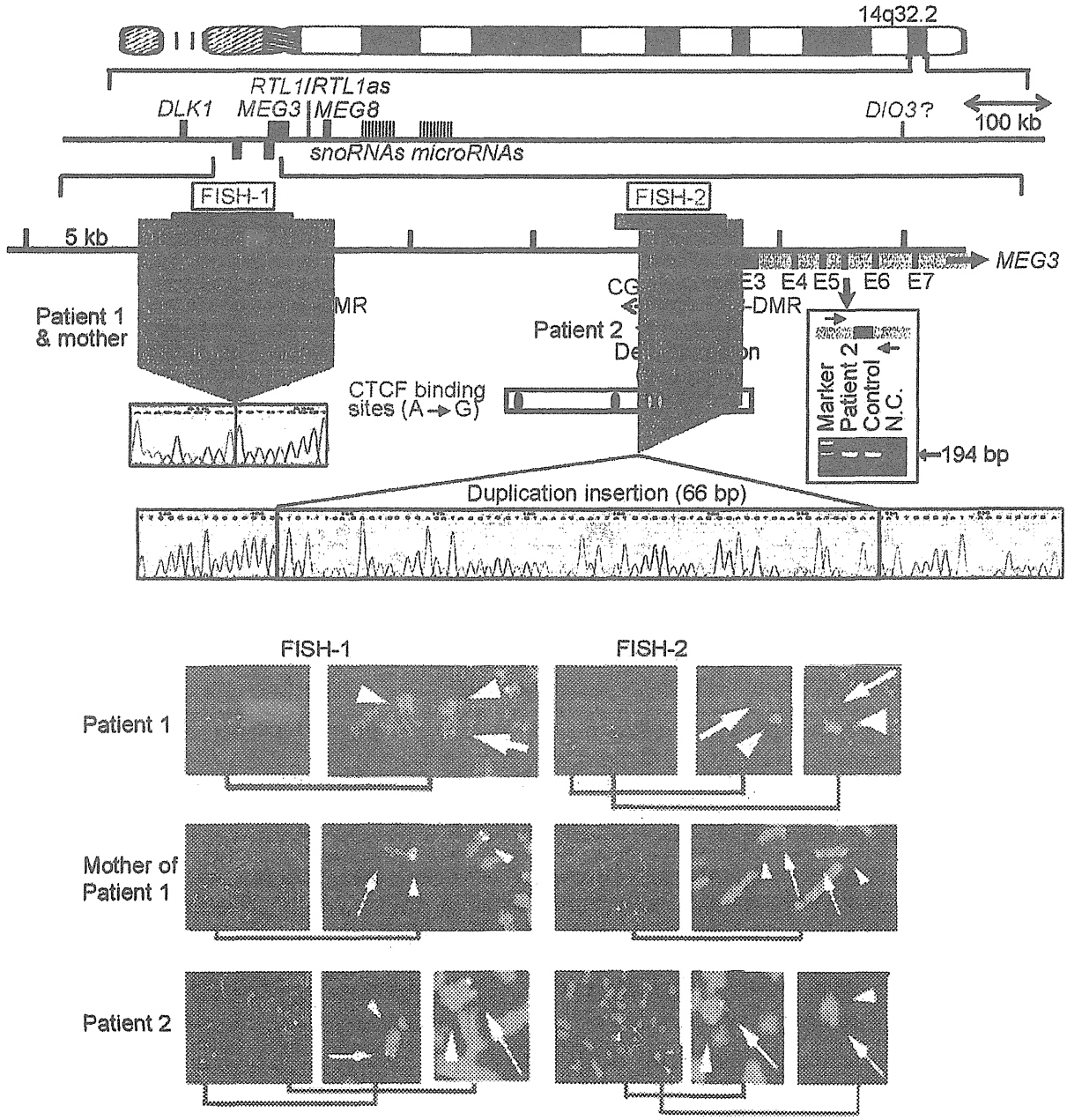

Figure 2. Physical map of the 14q32.2 imprinted region and the deleted segments in patient 1 and her mother and in patient 2 (shaded in gray). *PEGs* are shown in blue, *MEGs* in red, and the IG-DMR (CG4 and CG6) and the *MEG3*-DMR (CG7) in green. It remains to be clarified whether *DIO3* is a *PEG*, although mouse *Dio3* is known to be preferentially but not exclusively expressed from a paternally derived chromosome [35]. For *MEG3*, the isoform 2 with nine exons (red bars) and eight introns (light red segment) is shown (Ensembl; http://www.ensembl.org/index.html). Electrochromatograms represent the fusion point in patient 1 and her mother, and the fusion point accompanied by insertion of a 66 bp segment (highlighted in blue) with a sequence identical to that within *MEG3* intron 5 (the blue bar) in patient 2. Since PCR amplification with primers flanking the 66 bp segment at *MEG3* intron 5 has produced a 194 bp single band in patient 2 as well as in a control subject (shown in the box), this indicates that the 66 bp segment at the fusion point is caused by a duplicated insertion rather than by a transfer from intron 5 to the fusion point (if the 66 bp is transferred from the original position, a 128 bp band as well as a 194 bp band should be present in patient 2) (the marker size: 100, 200, and 300 bp). In the FISH images, the red signals (arrows) have been identified by the FISH-1 probe and the FISH-2 probe, and the light green signals (arrowheads) by the RP11-566I2 probe for 14q12 used as an internal control. The faint signal detected by the FISH-2 probe in patient 2 is consistent with the preservation of a ~1.2 kb region identified by the centromeric portion of the FISH-2 probe.
doi:10.1371/journal.pgen.1000992.g002

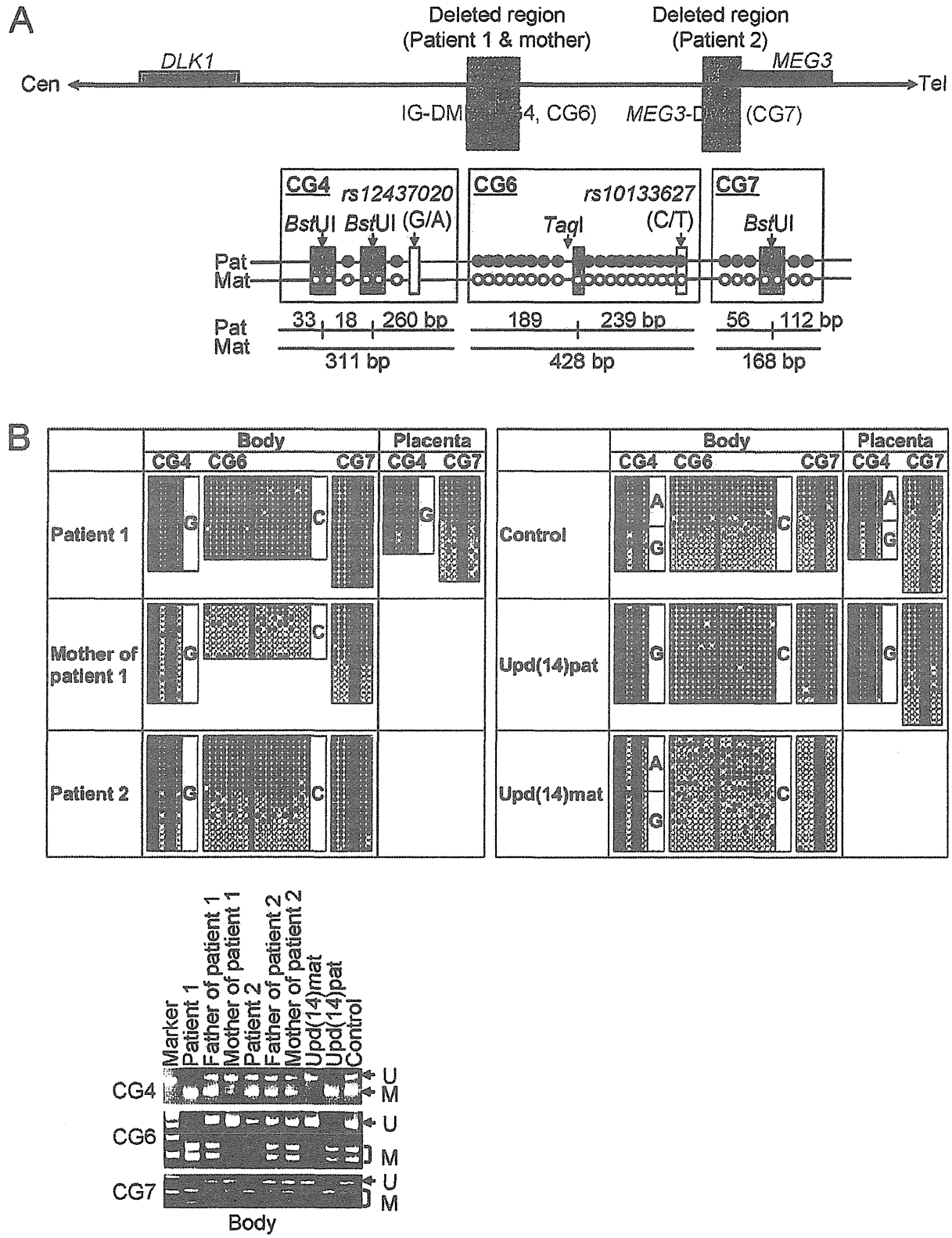

Figure 3. Methylation analysis of the IG-DMR (CG4 and CG6) and the *MEG3*-DMR (CG7). Filled and open circles indicate methylated and unmethylated cytosines at the CpG dinucleotides, respectively. (A) Structure of CG4, CG6, and CG7. Pat: paternally derived chromosome; and Mat:

maternally derived chromosome. The PCR products for CG4 (311 bp) harbor 6 CpG dinucleotides and a G/A SNP (*rs12437020*), and are digested with *Bst*UI into three fragment (33 bp, 18 bp, and 260 bp) when the cytosines at the first and the second CpG dinucleotides and the fourth and the fifth CpG dinucleotides (indicated with orange rectangles) are methylated. The PCR products for CG6 (428 bp) carry 19 CpG dinucleotides and a C/T SNP (*rs10133627*), and are digested with *Taq*I into two fragment (189 bp and 239 bp) when the cytosine at the 9th CpG dinucleotide (indicated with an orange rectangle) is methylated. The PCR products for CG7 harbor 7 CpG dinucleotides, and are digested with *Bst*UI into two fragment (56 bp and 112 bp) when the cytosines at the fourth and the fifth CpG dinucleotides (indicated with orange rectangles) are methylated. These enzymes have been utilized for combined bisulfite restriction analysis (COBRA). (B) Methylation analysis. Upper part shows bisulfite sequencing data. The SNP typing data are also denoted for CG4 and CG6. The circles highlighted in orange correspond to those shown in Figure 3A. The relatively long CG6 was not amplified from the formalin-fixed and paraffin-embedded placental samples, probably because of the degradation of genomic DNA. Note that CG4 is differentially methylated in a control placenta and is massively hypermethylated in a upd(14)pat placenta, whereas CG7 is rather hypomethylated in a upd(14)pat placenta as well as in a control placenta. Lower part shows COBRA data. U: unmethylated clone specific bands (311 bp for CG4, 428 bp for CG6, and 168 bp for CG7); and M: methylated clone specific bands (260 bp for CG4, 239 bp and 189 bp for CG6, and 112 bp and 56 bp for CG7). The results reproduce the bisulfite sequencing data, and delineate normal findings of the father of patient 1 and the parents of patient 2.
doi:10.1371/journal.pgen.1000992.g003

size was 8,558 bp (82,270,449–82,279,006 bp) for the microdeletion in patient 1 and her mother, and 4,303 bp (82,290,978–82,295,280 bp) for the microdeletion in patient 2. The microdeletion in patient 2 also involved the 5′ part of *MEG3* and five of the seven putative CTCF binding sites A–G [10], and was accompanied by insertion of a 66 bp sequence duplicated from *MEG3* intron 5 (82,299,727–82,299,792 bp on NT_026437). Direct sequencing of the exonic or transcribed regions detected no mutation in *DLK1*, *MEG3*, and *RTL1*, although several cDNA polymorphisms (cSNPs) were identified (Table S1). Oligoarray comparative genomic hybridization identified no other discernible structural abnormality (Figure S1B).

Methylation analysis of the two DMRs and the seven putative CTCF binding sites

We next studied methylation patterns of the previously reported IG-DMR (CG4 and CG6) and *MEG3*-DMR (CG7) (Figure 3A) [2], using bisulfite treated gDNA samples. Bisulfite sequencing and combined bisulfite restriction analysis using body samples revealed a hypermethylated IG-DMR and *MEG3*-DMR in patient 1, a hypomethylated IG-DMR and differentially methylated *MEG3*-DMR in the mother of patient 1, and a differentially methylated IG-DMR and hypermethylated *MEG3*-DMR in patient 2, and bisulfite sequencing using placental samples showed a hypermethylated IG-DMR and rather hypomethylated *MEG3*-DMR in patient 1 (Figure 3B).

We also examined methylation patterns of the seven putative CTCF binding sites by bisulfite sequencing (Figure 4A). The sites C and D alone exhibited DMRs in the body and were rather hypomethylated in the placenta (Figure 4B), as observed in CG7. Furthermore, to identify an informative SNP(s) pattern for allele-specific bisulfite sequencing, we examined a 349 bp region encompassing the site C and a 356 bp region encompassing the site D as well as a 300 bp region spanning the previously reported three SNPs near the site D, in 120 control subjects, the cases with upd(14)pat/mat, and patients 1 and 2 and their parents. Consequently, an informative polymorphism was identified for a novel G/A SNP near the site D in only a single control subject, and the parent-of-origin specific methylation pattern was confirmed (Figure 4C). No informative SNP was found in the examined region around the site C, and no other informative SNP was identified in the two examined regions around the site D, with the previously known three SNPs being present in a homozygous condition in all the subjects analyzed.

Expression analysis of the imprinted genes

Finally, we performed expression analyses, using standard reverse transcriptase (RT)-PCR and/or q-PCR analysis for multiple imprinted genes in this region (Figure 5A–5C). For leukocytes, weak expression was detected for *MEG3* and *SNORD114-29* in a control subject and the mother of patient 1 but not in patient 1. For skin fibroblasts, although all *MEGs* but no *PEGs* were expressed in control subjects, neither *MEGs* nor *PEGs* were expressed in patient 2. For placentas, although all imprinted genes were expressed in control subjects, *PEGs* only were expressed in patient 1. For the pituitary and adrenal of patient 2, *DLK1* expression alone was identified.

Expression pattern analyses using informative cSNPs revealed monoallelic *MEG3* expression in the leukocytes of the mother of patient 1 (Figure 5D), and biparental *RTL1* expression in the placenta of patient 1 (no informative cSNP was detected for *DLK1*) and biparental *DLK1* expression in the pituitary and adrenal of patient 2 (*RTL1* was not expressed in the pituitary and adrenal) (Figure 5E), as well as maternal *MEG3* expression in the control leukocytes and paternal *RTL1* expression in the control placentas (Figure S2). Although we also attempted q-PCR analysis, precise assessment was impossible for *MEG3* in the mother of patient 1 because of faint expression level in leukocytes and for *RTL1* in patient 1 and *DLK1* in patient 2 because of poor quality of mRNAs obtained from formalin-fixed and paraffin-embedded tissues.

Discussion

The data of the present study are summarized in Figure 6. Parental origin of the microdeletion positive chromosomes is based on the methylation patterns of the preserved DMRs in patients 1 and 2 and the mother of patient 1 as well as maternal transmission in patient 1. Loss of the hypomethylated IG-DMR of maternal origin in patient 1 was associated with epimutation (hypermethylation) of the *MEG3*-DMR in the body and caused paternalization of the imprinted region and typical upd(14)pat body and placental phenotypes, whereas loss of the hypomethylated *MEG3*-DMR of maternal origin in patient 2 permitted normal methylation pattern of the IG-DMR in the body and resulted in maternal to paternal epigenotypic alteration and typical upd(14)pat body, but no placental, phenotype. In this regard, while a 66 bp segment was inserted in patient 2, this segment contains no known regulatory sequence [11] or evolutionarily conserved element [12] (also examined with a VISTA program, http://genome.lbl.gov/vista/index.shtml). Similarly, while no control samples were available for pituitary and adrenal, the previous study in human subjects has shown paternal *DLK1* expression in adrenal as well as monoallelic *DLK1* and *MEG3* expressions in various tissues [11]. Furthermore, the present and the previous studies [2] indicate that this region is imprinted in the placenta as well as in the body. Thus, these results, in conjunction with the finding that the IG-DMR remains as a DMR and the *MEG3*-DMR exhibits a non-DMR in the placenta [2], imply the following: (1) the IG-DMR functions hierarchically as an upstream regulator for the methylation pattern of the *MEG3*-DMR on the maternally inherited chromosome in the body, but not in the placenta; (2) the hypomethylated

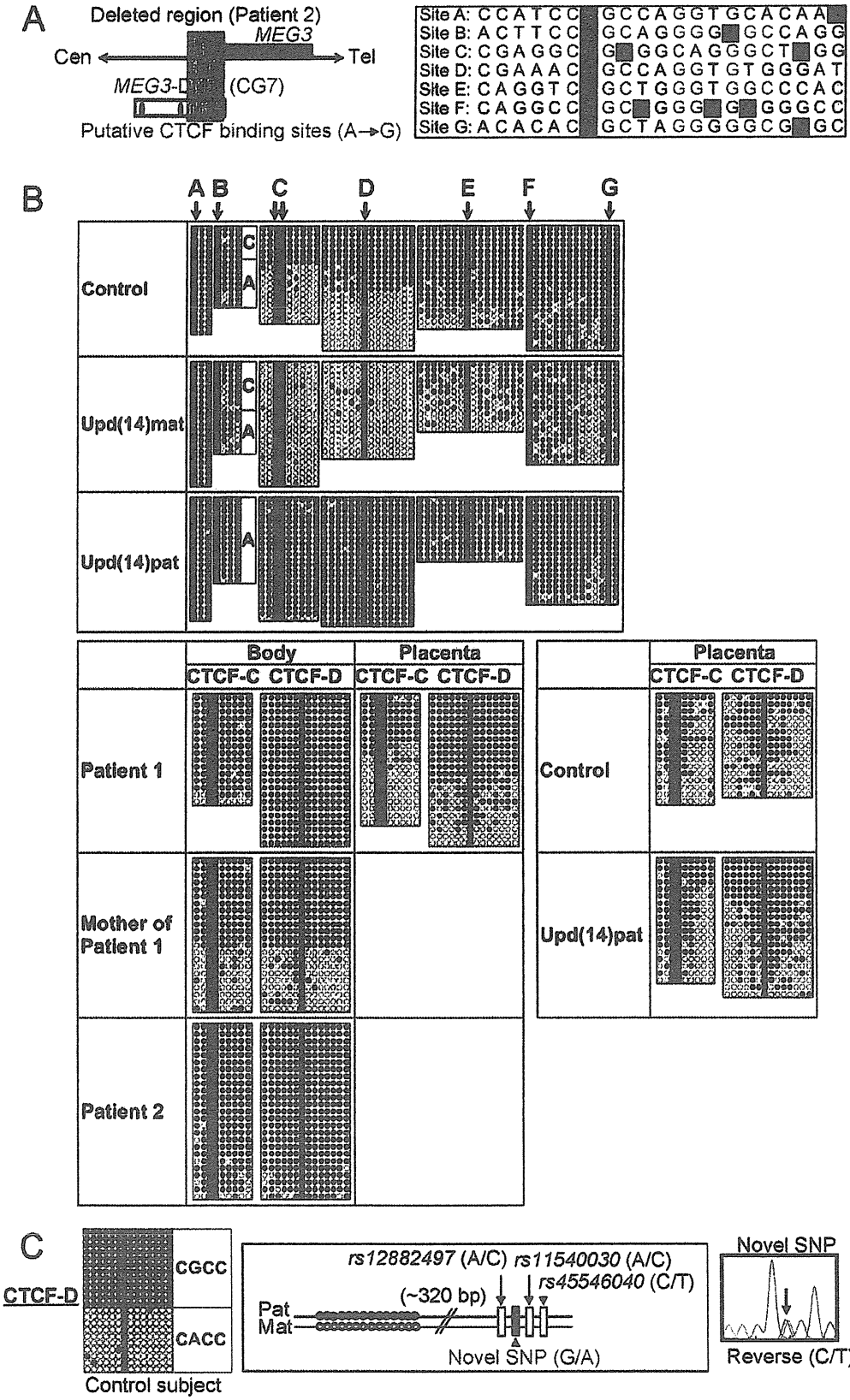
A
Deleted region (Patient 2)
MEG3
Cen
Tel
MEG3-D
(CG7)
Putative CTCF binding sites (A→G)
Site A: C C A T C C G C C A G G T G C A C A A
Site B: A C T T C C G C A G G G G C C A G G
Site C: C G A G G C G G G C A G G G C T G G
Site D: C G A A A C G C C A G G T G T G G G A T
Site E: C A G G T C G C T G G G T G G C C C A C
Site F: C A G G C C G C G G G G G G G C C
Site G: A C A C A C G C T A G G G G G C G G C
B
A B C D E F G
Control
Upd(14)mat
Upd(14)pat
Body
Placenta
CTCF-C CTCF-D
CTCF-C CTCF-D
Patient 1
Mother of Patient 1
Patient 2
Placenta
CTCF-C CTCF-D
Control
Upd(14)pat
C
CTCF-D
CGCC
CACC
Control subject
rs12882497 (A/C) rs11540030 (A/C)
rs45546040 (C/T)
(~320 bp)
Pat
Mat
Novel SNP (G/A)
Novel SNP
Reverse (C/T)

Figure 4. Methylation analysis of the putative CTCF protein binding sites A–G. (A) Location and sequence of the putative CTCF binding sites. In the left part, the sites C and D are painted in yellow and the remaining sites in purple. In the right part, the consensus CTCF binding motifs are shown in red letters; the cytosine residues at the CpG dinucleotides within the CTCF binding motifs are highlighted in blue, and those outside the CTCF binding motifs are highlighted in green [10]. (B) Methylation analysis. Upper part shows bisulfite sequencing data, using leukocyte genomic DNA samples. Since PCR products for the site B contain a C/A SNP (*rs11627993*), genotyping data are also indicated. The circles highlighted in blue correspond to those shown in Figure 4A. The sites C and D exhibit clear DMRs. Lower part indicates the results of the sites C and D using leukocyte and/or placental genomic DNA samples. The findings are similar to those of CG7. (C) Allele-specific methylation pattern of the CTCF binding site D. A novel G/A SNP has been identified in a single control subject, as shown on a reverse chromatogram delineating a C/T SNP pattern, while the previously reported three SNPs were present in a homozygous condition. Methylated and unmethylated clones are associated with the "G" and the "A" alleles, respectively.
doi:10.1371/journal.pgen.1000992.g004

MEG3-DMR functions as an essential imprinting regulator for both *PEGs* and *MEGs* in the body; and (3) in the placenta, the hypomethylated IG-DMR directly controls the imprinting pattern of both *PEGs* and *MEGs*. These notions also explain the epigenotypic alteration in the previous cases with epimutations or microdeletions affecting both DMRs (Figure S3).

It remains to be clarified how the IG-DMR and the *MEG3*-DMR interact hierarchically in the body. However, the present data, together with the previous findings in cases with epimutations [2,5–8], imply that *MEG3*-DMR can remain hypomethylated only in the presence of a hypomethylated IG-DMR and is methylated when the IG-DMR is deleted or methylated irrespective of the parental origin. Furthermore, mouse studies have suggested that the methylation pattern of the postfertilization-derived *Gtl2*-DMR (the mouse homolog for the *MEG3*-DMR) is dependent on that of the germline-derive IG-DMR [13]. Thus, a preferential binding of some factor(s) to the unmethylated IG-DMR may cause a conformational alteration of the genomic structure, thereby protecting the methylation of the *MEG3*-DMR.

It also remains to be elucidated how the IG-DMR and the *MEG3*-DMR regulate the expression of both *PEGs* and *MEGs* in the placenta and the body, respectively. For the *MEG3*-DMR, however, the CTCF binding sites C and D may play a pivotal role in the imprinting regulation. The methylation analysis indicates that the two sites reside within the *MEG3*-DMR, and it is known that the CTCF protein with versatile functions preferentially binds to unmethylated target sequences including the sites C and D [10,14–16]. In this regard, all the *MEGs* in this imprinted region can be transcribed together in the same orientation and show a strikingly similar tissue expressions pattern [1,12], whereas *PEGs* are transcribed in different directions and are co-expressed with *MEGs* only in limited cell-types [1,17]. It is possible, therefore, that preferential CTCF binding to the grossly unmethylated sites C and D activates all the *MEGs* as a large transcription unit and represses all the *PEGs* perhaps by influencing chromatin structure and histone modification independently of the effects of expressed *MEGs*. In support of this, CTCF protein acts as a transcriptional activator for *Gtl2* (the mouse homolog for *MEG3*) in the mouse [18].

Such an imprinting control model has not been proposed previously. It is different from the CTCF protein-mediated insulator model indicated for the *H19*-DMR and from the non-coding RNA-mediated model implicated for several imprinted regions including the KvDMR1 [19]. However, the KvDMR1 harbors two putative CTCF binding sites that may mediate non-coding RNA independent imprinting regulation [20], and the imprinting control center for Prader-Willi syndrome [21] also carries three CTCF binding sites (examined with a Search for CTCF DNA Binding Sites program, http://www.essex.ac.uk/bs/molonc/spa.html). Thus, while each imprinted region would be regulated by a different mechanism, a CTCF protein may be involved in the imprinting control of multiple regions, in various manners.

This imprinted region has also been studied in the mouse. Clinical and molecular findings in wildtype mice [1,22,23], mice with PatDi(12) (paternal disomy for chromosome 12 harboring this imprinted region) [13,24,25], and mice with targeted deletions for the IG-DMR (ΔIG-DMR) [22,26] and for the *Gtl2*-DMR (Δ*Gtl2*-DMR) [27] are summarized in Table 2. These data, together with human data, provide several informative findings. First, in both the human and the mouse, the IG-DMR is differentially methylated in both the body and the placenta, whereas the *MEG3/Gtl2*-DMR is differentially methylated in the body and exhibits non-DMR in the placenta. Second, the IG-DMR and the *MEG3/Gtl2*-DMR show a hierarchical interaction on the maternally derived chromosome in both the human and the mouse bodies. Indeed, the *MEG3/Gtl2*-DMR is epimutated in patient 1 and mice with maternally inherited ΔIG-DMR, and the IG-DMR is normally methylated in patient 2 and mice with maternally inherited Δ*Gtl2*-DMR. Third, the function of the IG-DMR is comparable between human and mouse bodies and different between human and mouse placentas. Indeed, patient 1 has upd(14)pat body and placental phenotypes, whereas mice with the ΔIG-DMR of maternal origin have PatDi(12)-compatible body phenotype and apparently normal placental phenotype. It is likely that imprinting regulation in the mouse placenta is contributed by some mechanism(s) other than the methylation pattern of the IG-DMR, such as chromatin conformation [22,28,29].

Unfortunately, however, the data of Δ*Gtl2*-DMR mice appears to be drastically complicated by the retained neomycin cassette in the upstream region of *Gtl2*. Indeed, it has been shown that the insertion of a *lacZ* gene or a neomycin gene in the similar upstream region of *Gtl2* causes severely dysregulated expression patterns and abnormal phenotypes after both paternal and maternal transmissions [30,31], and that deletion of the inserted neomycin gene results in apparently normal expression patterns and phenotypes after both paternal and maternal transmissions [31]. (In this regard, although a possible influence of the inserted 66 bp segment can not be excluded formally in patient 2, phenotype and expression data in patient 2 are compatible with simple paternalization of the imprinted region.) In addition, since the apparently normal phenotype in mice homozygous for Δ*Gtl2*-DMR is reminiscent of that in sheep homozygous for the callipyge mutation [32], a complicated mechanism(s) such as the polar overdominance may be operating in the Δ*Gtl2*-DMR mice [33]. Thus, it remains to be clarified whether the *MEG3/Gtl2*-DMR has a similar or different function between the human and the mouse.

Two points should be made in reference to the present study. First, the proposed functions of the two DMRs are based on the results of single patients. This must be kept in mind, because there might be a hidden patient-specific abnormality or event that might explain the results. For example, the abnormal placental phenotype in patient 1 might be caused by some co-incidental aberration, and the apparently normal placenta in patient 2 might be due to mosaicism with grossly preserved *MEG3*-DMR in the placenta and grossly deleted *MEG3*-DMR in the body. Second,

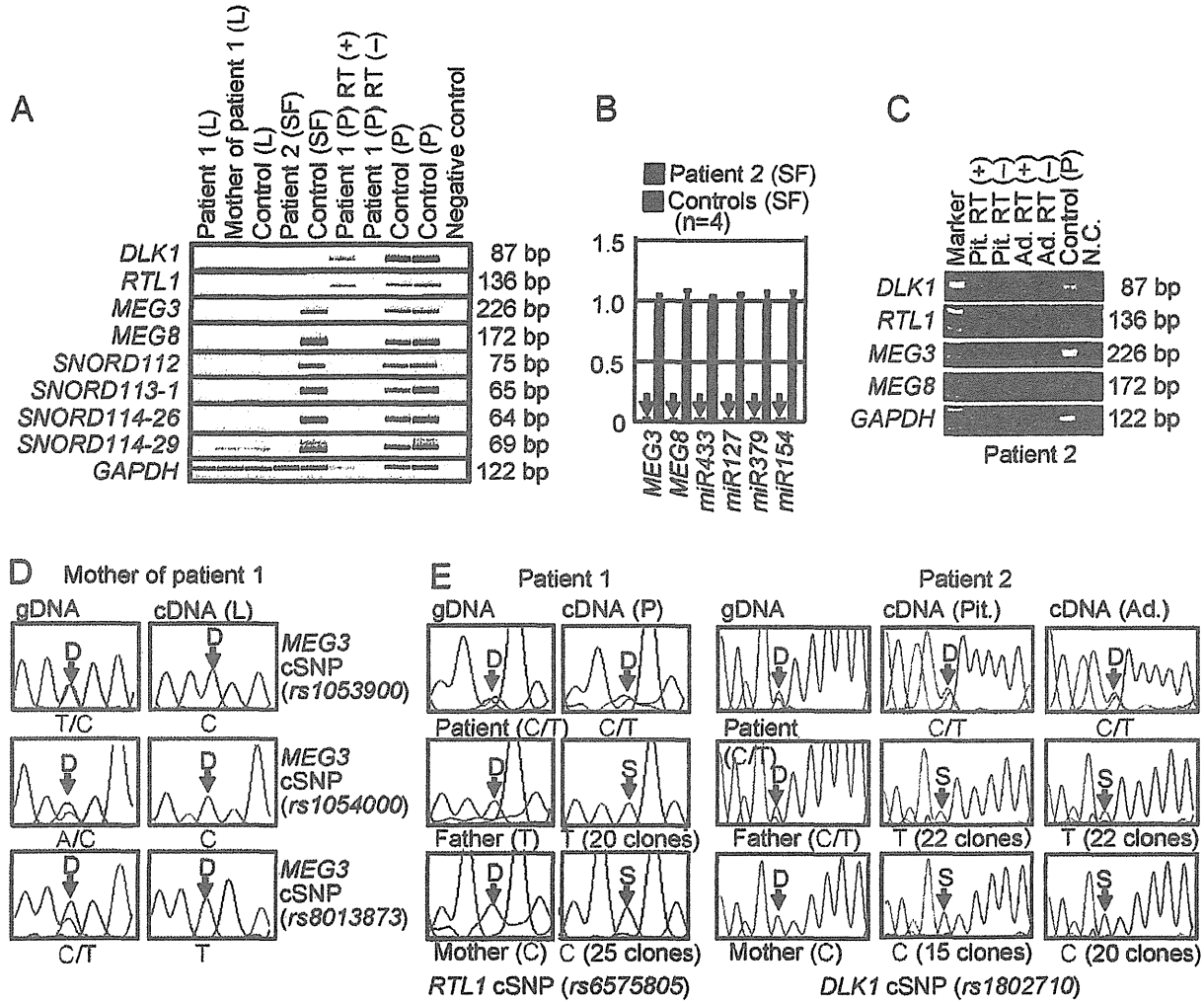

Figure 5. Expression analysis. (A) Reverse transcriptase (RT)-PCR analysis. L: leukocytes; SF: skin fibroblasts; and P: placenta. The relatively weak *GAPDH* expression for the formalin-fixed and paraffin-embedded placenta of patient 1 indicates considerable mRNA degradation. Since a single exon was amplified for *DLK1* and *RTL1*, PCR was performed with and without RT for the placenta of patient 1, to exclude the possibility of false positive results caused by genomic DNA contamination. (B) Quantitative real-time PCR (q-PCR) analysis of *MEG3*, *MEG8*, and *miRNAs*, using fresh skin fibroblasts (SF) of patient 2 and four control neonates. Of the examined *MEGs*, *miR433* and *miR127* are encoded by *RTL1as*. (C) RT-PCR analysis for the formalin-fixed and paraffin-embedded pituitary (Pit.) and the adrenal (Ad.) in patient 2. The bands for *DLK1* are detected in the presence of RT and undetected in the absence of RT, thereby excluding contamination of genomic DNA. (D) Monoallelic *MEG3* expression in the leukocytes of the mother of patient 1. The three cSNPs are present in a heterozygous status in gDNA and in a hemizygous status in cDNA. D: direct sequence. (E) Biparental *RTL1* expression in the placenta of patient 1 and biparental *DLK1* expression in the pituitary and adrenal of patient 2. D: direct sequence; and S: subcloned sequence. In patient 1, genotyping of *RTL1* cSNP (*rs6575805*) using gDNA indicates maternal origin of the "C" allele and paternal origin of the "T" allele, and sequencing analysis using cDNA confirms expression of maternally as well as paternally derived *RTL1*. Similarly, in patient 2, genotyping of *DLK1* cSNP (*rs1802710*) using gDNA denotes maternal origin of the "C" allele and paternal origin of the "T" alleles, and sequencing analysis using cDNA confirms expression of maternally as well as paternally inherited *DLK1*.
doi:10.1371/journal.pgen.1000992.g005

the clinical features in the mother of patient 1 such as short stature and obesity are often observed in cases with upd(14)mat (Table S2). However, the clinical features are non-specific and appear to be irrelevant to the microdeletion involving the IG-DMR, because loss of the paternally derived IG-DMR does not affect the imprinted status [2,26]. Indeed, *MEG3* in the mother of patient 1 showed normal monoallelic expression in the presence of the differentially methylated *MEG3*-DMR. Nevertheless, since the upd(14)mat phenotype is primarily ascribed to loss of functional *DLK1* (Figure S3B) [2,34], it might be possible that the microdeletion involving the IG-DMR has affected a *cis*-acting regulatory element for *DLK1* expression (for details, see Note in the legend for Table S2). Further studies in cases with similar microdeletions will permit clarification of these two points.

In summary, the results show a hierarchical interaction and distinct functional properties of the IG-DMR and the *MEG3*-DMR in imprinting control. Thus, this study provides significant advance in the clarification of mechanisms involved in the imprinting regulation at the 14q32.2 imprinted region and the development of upd(14) phenotype.

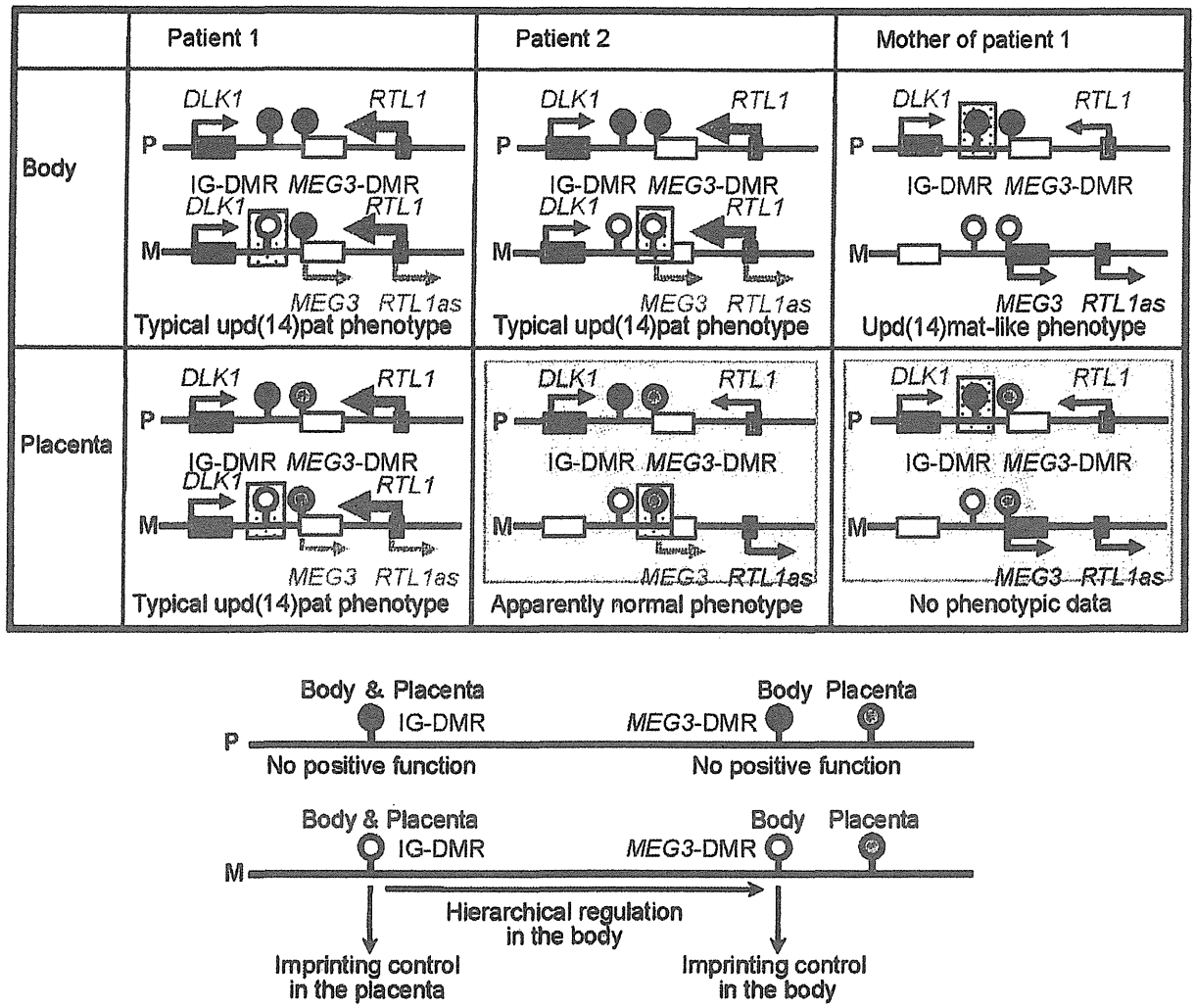

Figure 6. Schematic representation of the observed and predicted methylation and expression patterns. Deleted regions in patients 1 and 2 and the mother of patient 1 are indicated by stippled rectangles. P: paternally derived chromosome; and M: maternally derived chromosome. Representative imprinted genes are shown; these genes are known to be imprinted in the body and the placenta [2] (see also Figure S2). Placental samples have not been obtained in patient 2 and the mother of patient 1 (highlighted with light green backgrounds). Thick arrows for *RTL1* in patients 1 and 2 represent increased *RTL1* expression that is ascribed to loss of functional microRNA-containing *RTL1as* as a repressor for *RTL1* [26,36–38]; this phenomenon has been indicated in placentas with upd(14)pat and in those with an epimutation and a microdeletion involving the two DMRs (Figure S3A and S3C) [2]. *MEG3* and *RTL1as* that are disrupted or predicted to have become silent on the maternally derived chromosome are written in gray. Filled and open circles represent hypermethylated and hypomethylated DMRs, respectively; since the *MEG3*-DMR is rather hypomethylated and regarded as non-DMR in the placenta [2] (see also Figure 3), it is painted in gray.
doi:10.1371/journal.pgen.1000992.g006

Materials and Methods

Ethics statement

This study was approved by the Institutional Review Board Committees at National Center for Child health and Development, University College Dublin, and Dokkyo University School of Medicine, and performed after obtaining written informed consent.

Primers

All the primers utilized in this study are summarized in Table S3.

Sample preparation

For leukocytes and skin fibroblasts, genomic DNA (gDNA) samples were extracted with FlexiGene DNA Kit (Qiagen), and RNA samples were prepared with RNeasy Plus Mini (Qiagen) for *DLK1*, *MEG3*, *RTL1*, *MEG8* and *snoRNAs*, and with mirVana miRNA Isolation Kit (Ambion) for *microRNAs*. For paraffin-embedded tissues including the placenta, brain, lung, heart, liver, spleen, kidney, bladder, and small intestine, gDNA and RNA samples were extracted with RecoverAll Total Nucleic Acids Isolation Kit (Ambion) using slices of 40 μm thick. For fresh control placental samples, gDNA and RNA were extracted using ISOGEN (Nippon Gene). After treating total RNA samples with

Table 2. Clinical and molecular findings in wild-type and PatDi(12) mice and mice with maternally inherited ΔIG-DMR and Δ*Gtl2*-DMR.

	Wildtype	PatDi(12)	ΔIG-DMR (~4.15 kb)[a]	Δ*Gtl2*-DMR (~10 kb)[b]
				Neomycin cassette (+)
<Body>				
Phenotype	Normal	Abnormal[c]	PatDi(12) phenotype[c]	Normal at birth
				Lethal by 4 weeks
Methylation pattern				
IG-DMR	Differential	Methylated	Methylated[d]	Differential
Gtl2-DMR	Differential	Methylated	Epimutated[e]	Methylated[d]
Expression pattern				
Pegs	Monoallelic	Increased (~2x)	Biparental	Grossly normal
			Increased (2x or 4.5x)[f]	
Megs	Monoallelic	Absent	Absent	Decreased (<0.2~0.5x)[g]
<Placenta>				
Phenotype	Normal	Placentomegaly	Apparently normal	Not determined
Methylation pattern				
IG-DMR	Differential	Methylated	Not determined	Not determined
Gtl2-DMR	Non-DMR	Non-DMR	Not determined	Not determined
Expression pattern				
Pegs	Monoallelic	Not determined	Increased (1.5~1.8x)[g]	Decreased (0.5~0.85x)[g]
Megs	Monoallelic	Not determined	Decreased (0.6~0.8x)[g]	Decreased (<0.1~1.0)[g]
Remark			Paternal transmission[h]	Paternal transmission[i]
				Biparental transmission[j]

a The deletion size is smaller than that of patient 1 and her mother in this study, especially at the centromeric region.
b The microdeletion also involves *Gtl2*, and the deletion size is larger than that of patient 2 in this study.
c Body phenotype includes bell-shaped thorax with rib anomalies, distended abdomen, and short and broad neck.
d Hemizygosity for the methylated DMR of paternal origin.
e Hypermethylation of the maternally derived DMR.
f 2x *Dlk1* and *Dio3* expression levels and 4.5x *Rtl1* expression level. The markedly elevated *Rtl1* expression level is ascribed to a synergic effect between activation of the usually silent *Rtl1* of maternal origin and loss of functional microRNA-containing *Rtl1as* as a repressor for *Rtl1* [26,36–38].
g The expression level is variable among examined tissues and examined genes.
h The ΔIG-DMR of paternal origin has permitted normal *Gtl2*-DMR methylation pattern, intact imprinting status, and normal phenotype in the body (no data on the placenta).
i The Δ*Gtl2*-DMR of paternal origin is accompanied by normal methylation pattern of the IG-DMR and variably reduced *Pegs* expression and increased *Megs* expression in the body, and has yielded severe growth retardation accompanied by perinatal lethality.
j The homozygous mutants have survived and developed into fertile adults, despite rather altered expression patterns of the imprinted genes.
doi:10.1371/journal.pgen.1000992.t002

DNase, cDNA samples for *DLK1, MEG3, MEG8*, and *snoRNAs* were prepared with oligo(dT) primers from 1 μg of RNA using Superscript III Reverse Transcriptase (Invitrogen), and those for *microRNAs* were synthesized from 300 ng of RNA using TaqMan MicroRNA Reverse Transcription Kit (Applied Biosystems). For *RTL1*, cDNA samples were synthesized with *RTL1*-specific primers that do not amplify *RTL1as*. Control gDNA and cDNA samples were extracted from adult leukocytes and neonatal skin fibroblasts purchased from Takara Bio Inc. Japan, and from a fresh placenta of 38 weeks of gestation. Metaphase spreads were prepared from leukocytes and skin fibroblasts using colcemide (Invitrogen).

Structural analysis

Microsatellite analysis and SNP genotyping were performed as described previously [2]. For FISH analysis, metaphase spreads were hybridized with a 5,104 bp FISH-1 probe and a 5,182 bp FISH-2 probe produced by long PCR, together with an RP11-566I2 probe for 14q12 used as an internal control [2]. The FISH-1 and FISH-2 probes were labeled with digoxigenin and detected by rhodamine anti-digoxigenin, and the RP11-566I2 probe was labeled with biotin and detected by avidin conjugated to fluorescein isothiocyanate. For quantitative real-time PCR analysis, the relative copy number to RNaseP (catalog No: 4316831, Applied Biosystems) was determined by the Taqman real-time PCR method using the probe-primer mix on an ABI PRISM 7000 (Applied Biosystems). To determine the breakpoints of microdeletions, sequence analysis was performed for long PCR products harboring the fusion points, using serial forward primers on the CEQ 8000 autosequencer (Beckman Coulter). Direct sequencing was also performed on the CEQ 8000 autosequencer. Oligoarray comparative genomic hybridization was performed with 1×244K Human Genome Array (catalog No: G4411B) (Agilent Technologies), according to the manufacturer's protocol.

Methylation analysis

Methylation analysis was performed for gDNA treated with bisulfite using the EZ DNA Methylation Kit (Zymo Research). After PCR amplification using primer sets that hybridize both methylated and unmethylated clones because of lack of CpG

dinucleotides within the primer sequences, the PCR products were digested with appropriate restriction enzymes for combined bisulfite restriction analysis. For bisulfite sequencing, the PCR products were subcloned with TOPO TA Cloning Kit (Invitrogen) and subjected to direct sequencing on the CEQ 8000 auto-sequencer.

Expression analysis

Standard RT-PCR was performed for *DLK1*, *RTL1*, *MEG3*, *MEG8*, and *snoRNAs* using primers hybridizing to exonic or transcribed sequences, and one μl of PCR reaction solutions was loaded onto Gel-Dye Mix (Agilent). Taqman real-time PCR was carried out using the probe-primer mixtures (assay No: Hs00292028 for *MEG3* and Hs00419701 for *MEG8*; assay ID: 001028 for *miR433*, 000452 for *miR127*, 000568 for *miR379*, and 000477 for *miR154*) on the ABI PRISM 7000. Data were normalized against *GAPDH* (catalog No: 4326317E) for *MEG3* and *MEG8* and against *RNU48* (assay ID: 0010006) for the remaining *miRs*. The expression studies were performed three times for each sample.

To examine the imprinting status of *MEG3* in the leukocytes of the mother of patient 1, direct sequence data for informative cSNPs were compared between gDNA and cDNA. To analyze the imprinting status of *RTL1* in the placental sample of patient 1 and that of *DLK1* in the pituitary and adrenal samples of patient 2, RT-PCR products containing exonic cSNPs informative for the parental origin were subcloned with TOPO TA Cloning Kit, and multiple clones were subjected to direct sequencing on the CEQ 8000 autosequencer. Furthermore, *MEG3* expression pattern was examined using leukocyte gDNA and cDNA samples from multiple normal subjects and leukocyte gDNA samples from their mothers, and *RTL1* expression pattern was analyzed using gDNA and cDNA samples from multiple fresh normal placentas and leukocyte gDNA from the mothers.

Supporting Information

Figure S1 Structural analysis. (A) Quantitative real-time PCR analysis (q-PCR) for four regions (q-PCR-1-4) in patient 2. The q-PCR-1 and q-PCR-2 regions are present in two copies whereas q-PCR-3 and q-PCR-4 regions are present in a single copy in patient 2. The four regions are present in two copies in the parents and a control subject, in a single copy in the two previously reported patients with microdeletions involving the examined regions (Deletion-1 and Deletion-2 are case 2 and case 3 in Kagami et al. [2], respectively), and in three copies in a hitherto unreported case with 46,XX,der(17)t(14;17)(q32.2;p13)pat who have three copies of the 14q32.2 imprinted region. Since the microsatellite locus *D14S985* is present in two copies (Table S1) and the *MEG3*-DMR is deleted (Figure 2) in patient 2, this has served to localize the breakpoints. (B) Oligoarray comparative genomic hybridization for a ~1 Mb imprinted region. All the signals remain within the normal range (-1 SD ~ +1 SD) (shaded in light blue) in patients 1 and 2.
Found at: doi:10.1371/journal.pgen.1000992.s001 (1.17 MB TIF)

Figure S2 Expression analysis. (A) Maternal *MEG3* expression in the leukocytes of normal subjects. Genotyping has been performed for three cSNPs using genomic DNA (gDNA) and cDNA of leukocytes from control subjects and gDNA samples of their mothers, indicating that both maternally and non-maternally (paternally) derived alleles are delineated in the gDNA, whereas maternally inherited alleles alone are identified in cDNA. These three cSNPs have also been studied in the mother of patient 1 (Figure 5D). (B) Paternal *RTL1* expression in the placenta of a normal subject. Genotyping has been carried out for *RTL1* cSNP using gDNA and cDNA samples of a fresh placenta and gDNA sample from the mother, showing that both maternally and non-maternally (paternally) derived alleles are delineated in the gDNA, whereas a non-maternally (paternally) inherited allele alone is detected in cDNA. This cSNP has also been examined in the placenta of patient 1 (Figure 5E). Furthermore, the results confirm that the primers utilized in this study have amplified *RTL1*, but not *RTL1as*.
Found at: doi:10.1371/journal.pgen.1000992.s002 (0.39 MB TIF)

Figure S3 Schematic representation of the observed and predicted methylation and expression patterns in previously reported cases with upd(14)pat/mat-like phenotypes and in normal and upd(14)pat/mat subjects. For the explanations of the illustrations, see the legend for Figure 6. Previous studies have indicated that (1) Epimutation-1, Deletion-1, Deletion-2, and Deletion-3 lead to maternal to paternal epigenotypic alteration; (2) Epimutation-2 results in paternal to maternal epigenotypic alteration; and (3) Deletion-4 and Deletion-5 have no effect on the epigenotypic status [2,5–8,26]. (A) Cases with typical or mild upd(14)pat phenotype. Epimutation-1: Hypermethylation of the IG-DMR and the *MEG3*-DMR of maternal origin in the body, and that of the IG-DMR of maternal origin in the placenta (the *MEG3*-DMR is rather hypomethylated in the placenta) (cases 6–8 in Kagami et al. [2]). Deletion-1: Microdeletion involving *DLK1*, the two DMRs, and *MEG3* on the maternally inherited chromosome (case 2 in Kagami et al. [2]). Deletion-2: Microdeletion involving *DLK1*, the two DMRs, *MEG3*, *RTL1*, and *RTL1as* on the maternally inherited chromosome (cases 3 and 5 in Kagami et al. [2]). Deletion-3: Microdeletion involving the two DMRs, *MEG3*, *RTL1*, and *RTL1as* on the maternally inherited chromosome (case 4 in Kagami et al. [2]). These findings are explained by the following notions: (1) Epimutation (hypermethylation) of the normally hypomethylated IG-DMR of maternal origin directly results in paternalization of the imprinted region in the placenta and indirectly leads to paternalization of the imprinted region in the body via epimutation (hypermethylation) of the usually hypomethylated *MEG3*-DMR of maternal origin. Thus, the epimutation (hypermethylation) is predicted to have impaired the IG-DMR as the primary target, followed by the epimutation (hypermethylation) of the *MEG3*-DMR after fertilization; (2) Loss of the hypomethylated *MEG3*-DMR of maternal origin leads to paternalization of the imprinted region in the body; and (3) Loss of the hypomethylated IG-DMR of maternal origin results in paternalization of the imprinted region in the placenta. Furthermore, epigenotype-phenotype correlations imply that the severity of upd(14)pat phenotype is primarily determined by the *RTL1* expression dosage rather than the *DLK1* expression dosage [2]. (B) Cases with upd(14)mat-like phenotype. Epimutation-2: Hypomethylation of the IG-DMR and the *MEG3*-DMR of paternal origin (Temple et al. [5], Buiting et al. [6], Hosoki et al. [7], and Zechner et al. [8]). Deletion-4: Microdeletion involving *DLK1*, the two DMRs, and *MEG3* on the paternally inherited chromosome (cases 9 and 10 in Kagami et al. [2]). Deletion-5: Microdeletion involving *DLK1*, the two DMRs, *MEG3*, *RTL1*, and *RTL1as* on the paternally inherited chromosome (case 11 in Kagami et al. [2] and patient 3 in Buiting et al. [6]). These findings are consistent with the following notions: (1) Epimutation (hypomethylation) of the normally hypermethylated IG-DMR of paternal origin directly results in maternalization of the imprinted region in the placenta and indirectly leads to maternalization of the imprinted region in the body through epimutation (hypomethylation) of the usually hypermethylated *MEG3*-DMR of paternal origin. Thus, epimutation (hypomethylation) is predicted to have affected the IG-DMR